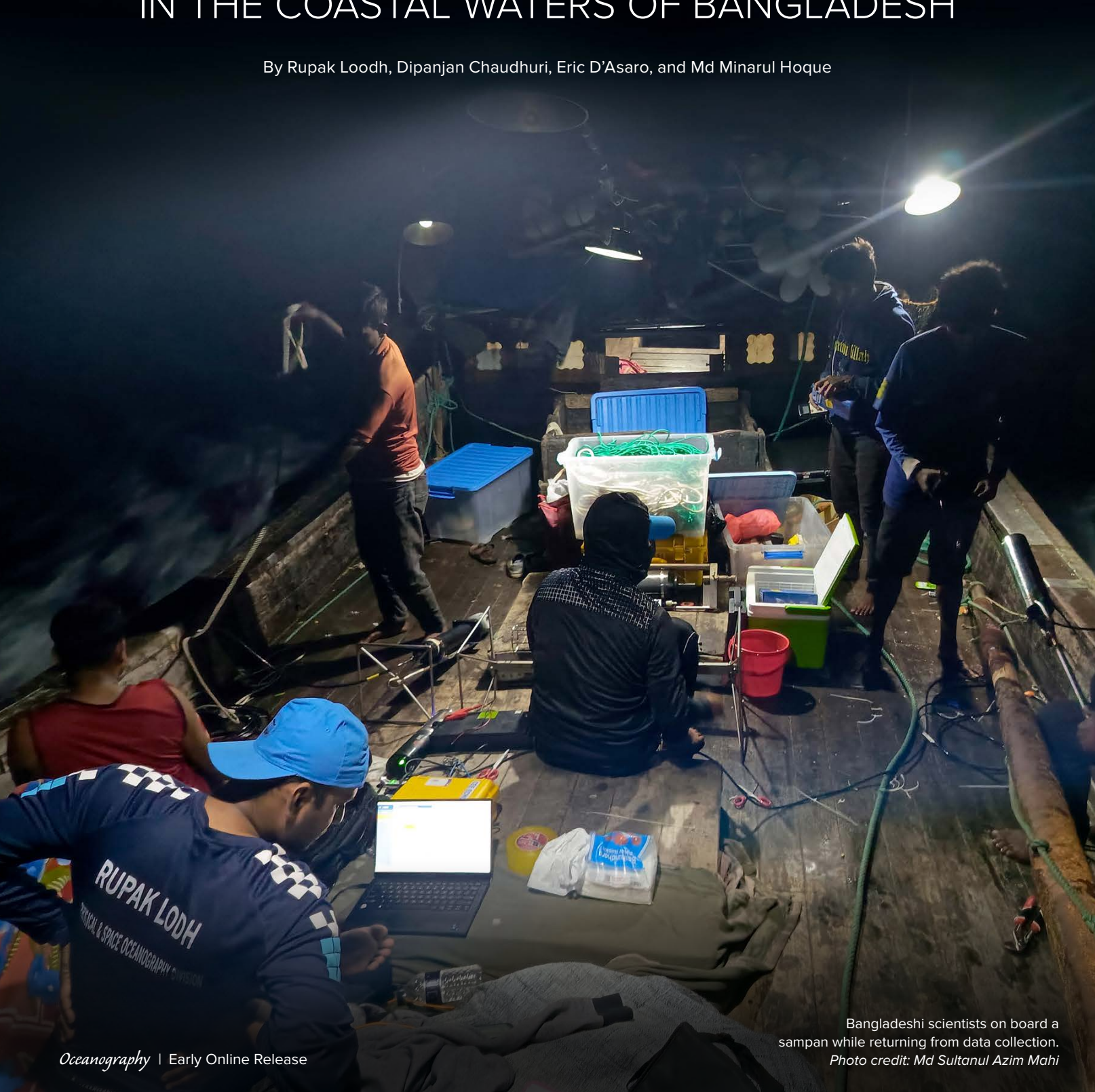
# COST-CONSCIOUS MEASUREMENTS

IN THE COASTAL WATERS OF BANGLADESH



**ABSTRACT.** The northern Bay of Bengal plays a crucial role in regional climate, human activities, and ecological diversity, but it is unstudied by oceanographers. In 2022, the Bangladesh Oceanographic Research Institute began to address this important problem by initiating a project to collect in situ data off the coast of Cox's Bazar, Bangladesh. We report the initial results from winter 2022–23 here. High-resolution spatial measurements of ocean temperature, salinity, and horizontal velocities were made using modern sensors adapted to local boats. During this period, the coastal seas display sharp salinity-dominated density fronts, prominent temperature inversions, and partially compensated water masses. We hypothesize that these characteristics result from the stirring and mixing of cold and fresh water from local rivers, and warm and salty water from the central Bay of Bengal, creating distinct water masses on the Bangladeshi shelf. Future work aims to continue to modernize the capabilities of Bangladeshi oceanography through international collaborations, emphasizing state-of-the-art instrumentation, experimental design, and data analysis. These activities combine in a novel "cost-conscious oceanography" approach, pointing toward an innovative solution for the Global South to address data gaps in uncharted coastal seas.

# **INTRODUCTION**

## **BAY OF BENGAL**

The South Asian Monsoon impacts the livelihoods of one-fourth of the world's population, particularly those living around the Bay of Bengal (BoB). The seasonal rainfall and river inflows contribute significant freshwater flux of 1.6 m yr<sup>-1</sup> (Bhat et al., 2001; Vinayachandran et al., 2002; Sengupta et al., 2006), resulting in the development of a thin, salinity-stratified surface layer in the northern and central BoB (Figure 1a). This layer has two important effects: (1) it increases the number of monsoonal convective systems that deliver rain to central India (Waliser et al., 2003; Goswami, 2012; Samanta et al., 2018), and (2) it contributes to the intensification of destructive tropical cyclones in the BoB (Sengupta et al., 2008; Balaguru et al., 2012, 2014; Neetu et al., 2012; Chaudhuri et al., 2019).

Furthermore, the BoB is vital for controlling maritime access to the Far East, affecting major shipping routes that facilitate 25% of global trade. Given its growing strategic importance, key stakeholders such as the United States, China, India, and Japan are making substantial investments to ensure the maritime security and stability that is essential for maintaining a continuous flow of energy resources and trade opportunities (Chaudhury and Pant, 2024; Ranjan and Attanayake, 2024).

# **OCEAN OBSERVING NETWORK**

A network of BOB moored buoys (Figure 1d) includes, at any given time, approximately six Ocean Moored buoy Network for Northern Indian Ocean (OMNI) buoys (including one in the Andaman Sea) that are maintained by the National Institute of Ocean Technology (NIOT) of India (Venkatesan et al., 2013), along with four RAMA

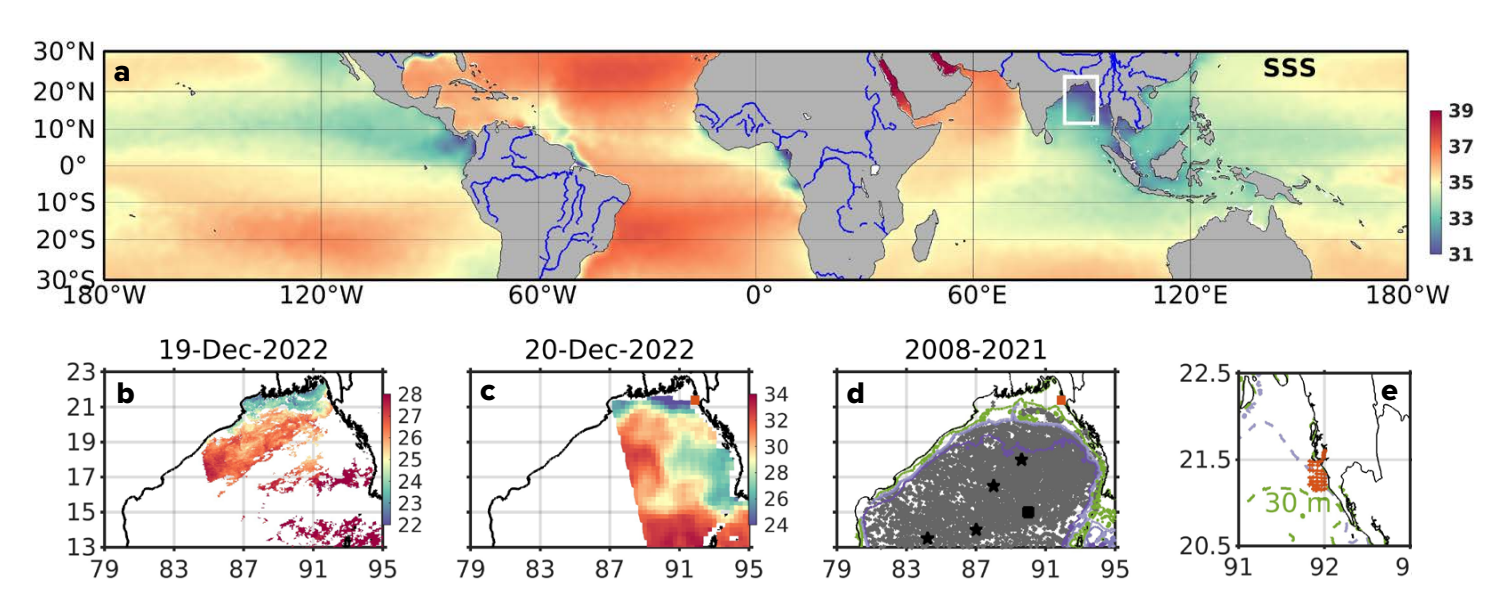


FIGURE 1. (a) Annual mean sea surface salinity from the World Ocean Atlas 2018 (WOA18; Garcia et al., 2019). The white square locates the Bay of Bengal. (b) Daytime 4 km resolution NOAA/Advanced Very High Resolution Radiometer (AVHRR) sea surface temperature (SST, °C) is plotted for December 19, 2022; blank white areas are clouds. (c) Daytime pass of Soil Moisture Active Passive Satellite (SMAP) swath over the Bay of Bengal on December 20, 2022. (d) Map showing the locations of Argo floats during 2008–2021 (gray) in the Bay of Bengal. The green line shows the 50 m depth contour, and the blue lines indicate 3000 m, 2000 m, 1000 m, and 500 m depths. Four black stars and a square indicate the positions of the buoys maintained by the National Institute of Ocean Technology (NIOT) and NOAA's Pacific Marine Environmental Laboratory in the Bay of Bengal. The red square in the head bay represents the sampling area within the unexplored continental shelf near the city of Cox's Bazar. (e) In this zoom into the coastal sampling area, red dots indicate the locations of 60 CTD stations taken during 2021–2022 by the Bangladesh Oceanographic Research Institute (BORI) that are discussed here. Green and blue dashed lines plot depth contours of 30 m and 10 m, respectively.

(Research Moored Array for African-Asian-Australian Monsoon Analysis and Prediction) moorings operated by the US National Oceanic and Atmospheric Administration (NOAA) in collaboration with India (McPhaden et al., 2009). These buoys collect high-resolution data on upper ocean conditions, including temperature, salinity (conductivity), currents at various depths, and surface meteorological data such as wind, humidity, pressure, temperature, rainfall, and radiation. Some buoys also collect wave

interference in multiple microwave channels following the outbreak of civil war in Myanmar.

Coastal seas also lack depth-resolved in situ temperature and salinity measurements, as robotic floats, such as those in the international Argo program, require a parking depth of 1,000 m (Roemmich et al., 2009) and cannot operate in such shallow depths as those around Cox's Bazar. (However, a few Argo floats that have entered the northern BoB continental shelf [Figure 1d] have pro-

The first area of success encompasses the development of an indigenous method for measuring coastal oceans with modern sensors and the collection of unprecedented data in uncharted waters by Bangladeshi scientists

parameters. In addition, India organizes several scientific oceanographic cruises yearly to enhance understanding of the interactions between oceanic and atmospheric processes that affect climate, extreme weather events, ecosystems, and human populations.

The US Office of Naval Research (ONR), in collaboration with India, Sri Lanka, Thailand, and the Maldives, has conducted three significant observational programs in the BoB over the past 10 years (Wijesekera et al., 2016; Shroyer et al., 2021). These programs primarily took place in international waters below 20°N, notably excluding two key countries, Bangladesh and Myanmar. As a result, the northeastern portion of the BoB remains one of the unexplored frontiers of our planet, holding immense potential for future research and discovery. It is an "aqua incognito."

### **MOTIVATION**

Bangladesh is a riverine country located on the northern coast of the BoB. It encompasses the confluence of the Ganges, Brahmaputra, and Meghna Rivers, which discharge substantial amounts of fresh water (about 0.04 Sv) into the vast and relatively flat waters of the northeastern Bengal shelf. Modern physical oceanography increasingly relies on satellite remote sensing for continuous ocean sampling. However, clouds can hinder the retrieval of infrared sea surface temperature (SST) data in coastal areas (Figure 1b). Although microwave remote sensing is not affected by cloud cover, satellite-derived, microwave-based SST measurements are often compromised by land contamination due to antenna side lobes within approximately 50 km of the coast (Wentz et al., 2000; Donlon et al., 2007; Pearson et al., 2018). Furthermore, sea surface salinity measurements obtained through satellite remote sensing may exhibit significant systematic errors near coastal regions (Figure 1c) and in areas affected by radio frequency interference (Boutin et al., 2021). Recently, salinity data from NASA's Soil Moisture Active Passive Satellite (SMAP) were contaminated throughout the BoB, likely due to radio frequency vided valuable information about water mass characteristics).

These factors result in the poor understanding of the north continental shelf of the BoB that motivates the effort described here to collect more data in this region.

In 2020, the Bangladesh Oceanographic Research Institute (BORI) launched a coastal observation program to tackle the challenges associated with coastal oceanography research. The Bangladesh Government supports this program to establish sustained monitoring of several oceanic variables. Under the framework of the blue economy, BORI's continuous efforts across all branches of oceanography hold promise for discovering potential resources for fisheries and renewable energy from ocean sources.

# **STUDYING THE AQUA INCOGNITO**

Our study focuses on the northern coastal area of the BoB near the city of Cox's Bazar, located approximately 120 km south of the Karnaphuli River and 200 km southeast of the Ganga-Brahmaputra-Megna River mouth (Figure 1e). We chose this site because of its proximity to the institute, which facilitates logistics movements and local support. Because BORI has no seagoing ocean vessel, we rely on local fishing boats. So far, our observations have only been possible during winter as the sea becomes too rough during the southwest summer monsoon.

#### **BOAT**

Our sampling was conducted using a wooden fishing boat (locally called a sampan) of a type that is ubiquitous in the Cox's Bazaar coastal area (Figure 2a); ten to 15 fishermen usually fish for seven to 10 days using sampans. The choice of this boat was based on its suitability for the local conditions and its stability in the water. It is 12.8 m in length, with a maximum width of 3.66 m and a draft of 2.1 m. Powered by a 32 HP engine, the boat cruises at 9 km per hour and has a carrying capacity of 12 tons. Sampling trips usually commence at 7 a.m. local time and return at sunset at 5 p.m.,

covering roughly 100 km and 10 sampling stations. The daily cost of using the boat is about \$400.

At each sampling station, the boat driver (locally called majhee) skillfully stabilized the boat using the Global Positioning System (GPS) position, ensuring a smooth sampling process. We utilized Android-based GPS software, specifically GeoTracker and Google Maps, which offer an accuracy range of 3 m to 10 m. We use premarked nylon rope with a depth indicator and an echo sounder for depth information. After each conductivity-temperature-depth (CTD) and acoustic Doppler current profiler (ADCP) operation, we extract data from the sensor and conduct a data quality check on the boat, ensuring the accuracy and credibility of our results. The average rolling and pitching at each station measured by the inbuilt motion sensor in the Aquadopp ADCP are 10° and 12°, respectively, suggesting calm sea conditions and a stable boat.

#### **INSTRUMENTS AND METHODS**

After extensive discussions, we carefully selected the instruments to be used in this study. Our main focus was to ensure that the chosen instruments were all usable from an ordinary fishing boat without a deployment platform and that had proven reliability. All instruments were procured under BORI's Research & Development project 2020-2022, with recommendations from an expert committee comprised of experienced oceanographic scientists. Table 1 lists detailed information about each instrument. The total cost for procuring all the instruments was approximately \$50,000 USD.

Our study used two CTD sensors: the CTD90M from Sea & Sun Technology and the Star-Oddi sensor. The CTD90M, known for its high quality and accuracy, was our primary instrument for calibrating the other CT sensors. Its conductivity cell features a naturally flushed design similar to the RBR Concertos "combined CT" cell, which has a co-located temperature sensor (Pt100). We selected continuous profiling modes, acquiring data at seven samples per second. The CTD profiles were secured to a steel cage with a 1.7-liter Niskin water sampler. Our team of technicians and scientists deployed and recovered the CTD by hand for each cast from the side of the vessel, using pre-labeled nylon rope for assistance (Figure 2b).



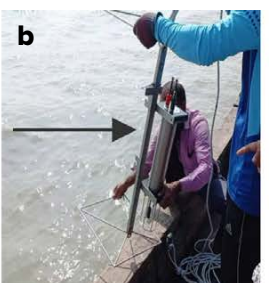






FIGURE 2. These photos show the platform, instruments, and data collection procedure used in this study. Gray arrows point to (a) the fishing boat used, (b) CTD sensors, (c) an ADCP, and (d) a thermosalinograph.

**TABLE 1.** List of instruments.

EQUIPMENT	MAKE/MODEL	PARAMETER	RESOLUTION	ACCURACY	RANGE
CTD90M	Sea & Sun Technology	Temperature	0.0005°C	±0.002°C	-2-60°C
		Conductivity	0.005 mS cm <sup>-1</sup>	±0.01 mS cm <sup>-1</sup>	0-300 mS cm <sup>-1</sup>
		Pressure	0.002% FS	0.05% FS	0–200 bar
DST CT	Star-Oddi	Temperature	0.032°C	±0.1°C	−1−40°C
		Conductivity	0.03 mS cm <sup>-1</sup>	±0.1 mS cm <sup>-1</sup>	3–68 m S cm <sup>-1</sup>
Aquadopp 600 kHz	Nortek	Zonal meridional velocity	1 cm s <sup>-1</sup>	±1% of the measured value	±5.75 m s <sup>-1</sup>
Niskin-Type Plastic Water Sampler	HYDRO-BIOS				

Over a span of five days, the team successfully collected 57 profiles. The average descent and ascent rate of the CTD frame was 0.07 m s<sup>-1</sup>, with each complete CTD operation taking approximately 6 to 8 minutes. We processed each CTD profile by averaging data at 25 cm intervals. Slight differences in temperature and salinity values were observed between the upcast and downcast profiles, probably due to advection. Because we did not have a commercial thermosalinograph installed on a dedicated research vessel, we innovatively developed a new method to measure finescale horizontal gradients of near-surface temperature and salinity. First, we placed one conductivity/temperature logger, along with one temperature logger manufactured by Star-Oddi, inside a small cage made of satin stainless steel. These compact sensors, which are high-pressure tolerant and have long battery lives, are among the smallest CT loggers on the market, measuring less than 5 cm.

Next, for flotation, we attached the cage to two five-liter plastic containers. Finally, we deployed the setup behind the boat using a 20-meter-long rope, which helped us avoid the wake generated by the boat. We used a depressor weight attached to a one-meter-long rope connected to the cage to ensure the sensors remained submerged while towing. We called this arrangement the "cost-conscious thermosalinograph" (Figure 2d). The sensors were programmed to record data at two-minute intervals, resulting in a fine horizontal resolution of 150 m for temperature and salinity in the upper 1 m of the water column.

We used the Aquadopp 600 kHz ADCP to measure the horizontal velocities in the upper ocean. At each CTD station, we securely mounted the ADCP on a pole extending over the side of the boat, facing downward (Figure 2c). The ADCP was deployed at a depth of 2 m and was configured to sample in 1 m vertical bins with a 1 sec sampling interval. We processed the velocity data using Nortek's AquaPro software. To minimize measurement error, we averaged all the velocity data over a period of five to 10 minutes.

# **RESULTS**

# **COASTAL MEASUREMENTS**

Figure 3a,b shows the surface temperature and salinity in Bangladesh's coastal waters on five days: December 19, 22, 23, and 24 in 2022 and January 14, 2023. The northern waters, influenced by riverine sources, are colder (24°C compared to 29°C) and less saline (12 psu compared to 32 psu) than those in the southern part of the study. The depth-averaged currents flow from the south, bringing warmer and saltier water to the region (see Figure 3c).

Strong stratification is observed in northern waters, with an average buoyancy frequency  $(N^2)$  of  $10^{-3}$  s<sup>-2</sup> at depths of 2–4 m (Figure 3g). In contrast, the southern waters show evidence of well-mixed conditions. The data also indicate a temperature inversion north of 22°N (Figure 3d), where the subsurface layers are warmer than the surface. This phenomenon is consistent with previous studies (Vinayachandran et al., 2002; Thadathil et al., 2016; Masud-Ul-Alam et al., 2022) and is particularly pronounced within the upper 10 m of the water column.

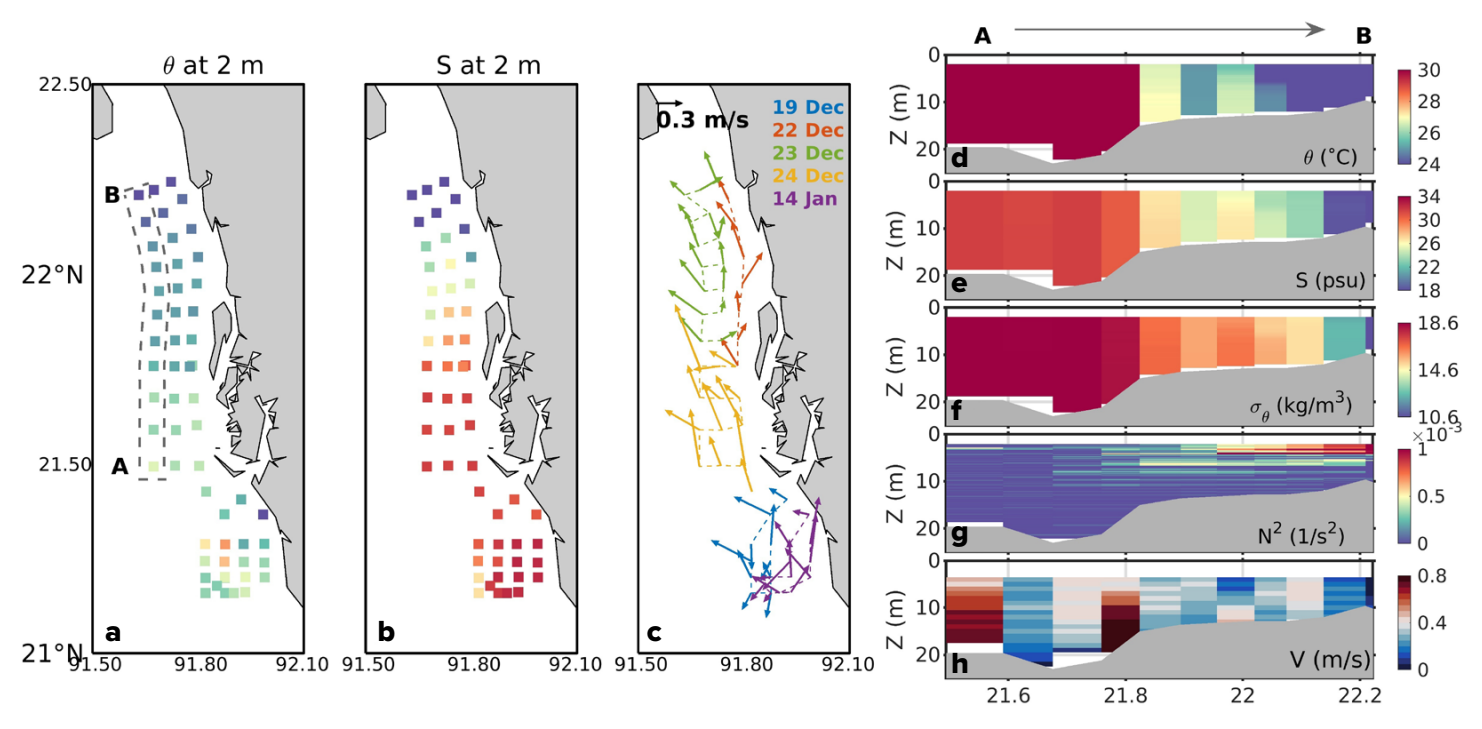


**FIGURE 3.** (a) Temperature and (b) salinity measurements taken at a depth of 2 m. (c) Flow patterns along the Cox's Bazar coast during the measurement periods, with different colors representing different days. Depth-latitude profiles are plotted along A to B within the dashed-line box in panel a for (d) potential temperature ( $\theta$ , °C), (e) salinity (S, psu), (f) potential density ( $\sigma_{\theta}$ , kg m<sup>-3</sup>), (g) square of the Brunt-Väisälä buoyancy frequency ( $N^2$ ,  $S^{-2}$ ), and (h) meridional velocity (V m s<sup>-1</sup>) as measured on December 23 and 24, 2022.

The inversion primarily arises from surface cooling associated with the "Western Disturbance" (Dimri and Chevuturi, 2016). In a shallow mixed layer, like the one observed here, much of the incoming atmospheric heat escapes into the subsurface ocean as shortwave radiation, which further intensifies the temperature inversion. Notably, salinity plays a more critical role than temperature in influencing the stability of the water column (Figure 3e–g). Throughout the recorded data, distinct temperature and salinity fronts are visible, raising intriguing questions about mixing processes and thermodynamics in this region.

# **OBSERVATIONS ON DECEMBER 19, 2022**

We present evidence of partially density-compensated submeso-scale surface fronts (Figure 4c,d) with lateral scales ranging from 1 km to 10 km, based on in situ observations in the coastal region, along with NOAA Visible Infrared Imaging Radiometer Suite (VIIRS) satellite SST data with a resolution of  $0.12 \times 0.9$  km. A notable observation by the satellite recorded at 1 a.m. local time on December 20, 2022, reveals a 50 km filament of warm water located just east and south of the coasts of Bangladesh and Myanmar (see Figure 4a,b). This warm filament is approximately

5 km wide and has an SST 2°C higher than the surrounding waters. The northern side of the filament has a mushroom-like appearance and forms a front with the incoming colder river water. Although we collected data in the area eight hours before the satellite passed (Figure 4b), the filament remained in place, suggesting that mixing occurs slowly.

Temperature-salinity (T-S) plots at various depths and different latitudes (Figure 4c,d) show two distinct water masses in the coastal waters of Bangladesh during winter. The northern water is primarily "minty" (Jackett and McDougall, 1985; Flament, 2002), meaning it is cold (24°C) and fresh (12 psu) river water that has been carried along the coast. As it moves, it mixes with the "spicy" warm (29°C) and salty (32 psu) waters of the BoB, resulting in the formation of different types of coastal water (Figure 4c,d). A combination of vertical (M1and M2 in Figure 4c) and horizontal mixing (M3 in Figure 4c) can explain the distribution of temperature and salinity on the continental shelf. Vertical mixing occurs on the surface or bottom, probably due to surface cooling or tidal influences, while intermediate depths are more susceptible to horizontal mixing (Figure 4c,d).

<sup>&</sup>lt;sup>1</sup> In oceanography, "spice" describes water masses with varying salinity and temperature along isopycnals, measured in density units and nearly orthogonal to potential density. Cold and fresh water is called "minty," while warm and salty water is known as "spicy," both having the same density.

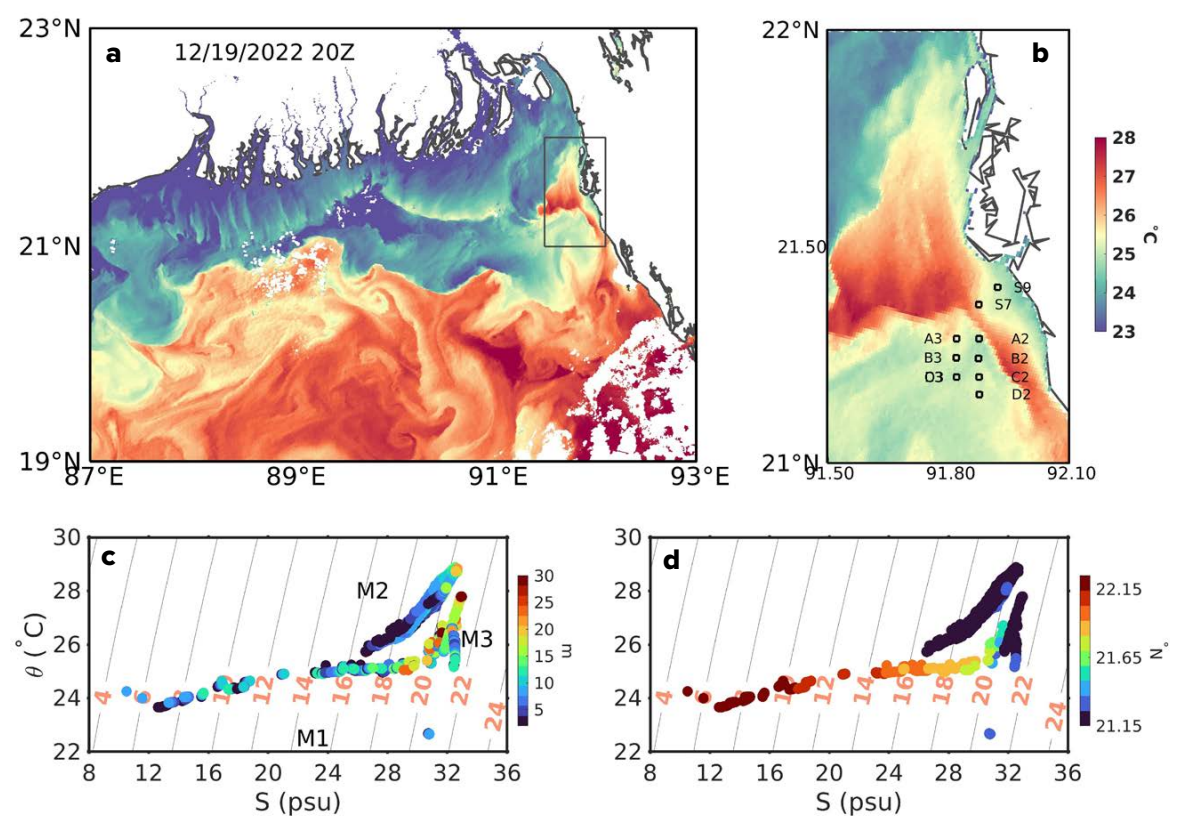


**FIGURE 4.** (a) NOAA Visible Infrared Imaging Radiometer Suite (VIIRS) SST (°C) for January 19, 2022. Blank areas are clouds or land. (b) A magnified view shows SST in the vicinity of the Bangladesh coast near Cox's Bazar. CTD locations are marked by squares. The evolution of temperature and salinity (TS) in the coastal ocean is shown with colors indicating (c) measurement depths and (d) latitudes. The three straight lines labeled M1, M2, and M3 represent resultant water masses formed due to the mixing of minty river water and spicy ocean water.

#### LATERAL VARIATIONS AND FRONTS ALONG BOAT TRACK

Our measurements on December 19, 2022, began at 7 a.m. local time, continued until 5 p.m., and were made in a 60 km rectangular loop (Figure 5a). That day, we completed a time series of measurements of vertical profiles, including temperature, salinity, and horizontal velocities at 10 different stations (Figure 5a). We deployed our cost-conscious thermosalinograph behind our boat to capture the initial insights into horizontal temperature and salinity variability. The thermosalinograph collected continuous data, and a comparison with near-surface temperature and salinity from the CTD instrument indicates that the salinity measurements from the thermosalinograph are generally reliable (Figure 5f,g). Note that we used different sampling patterns during the other four days (see Figure 4c).

On December 19, 2022, the along-track temperature and salinity measurements indicate that we crossed two prominent sharp fronts (Figure 5b–d). The data show that coastal waters are the coldest and saltiest, measuring 24°C and 30 psu, while the waters farther away are warmer and fresher, at 26°C and 26.5 psu. Between these zones, we find the warmest and saltiest waters, with a temperature of 27°C and a salinity of 31.5 psu (Figure 5b–d).

Horizontal density gradients are prevalent throughout the measurement period, reaching a minimum within the first 20 km (along-track distance) off the coast due to temperature and salinity compensation (Figure 5d,e). In contrast, a sharp, dynamically active front is observed farther from the coast (between 20 to 30 km) with a significant lateral density difference of 4 kg m<sup>-3</sup> over a spatial scale of 4 km. These observations suggest

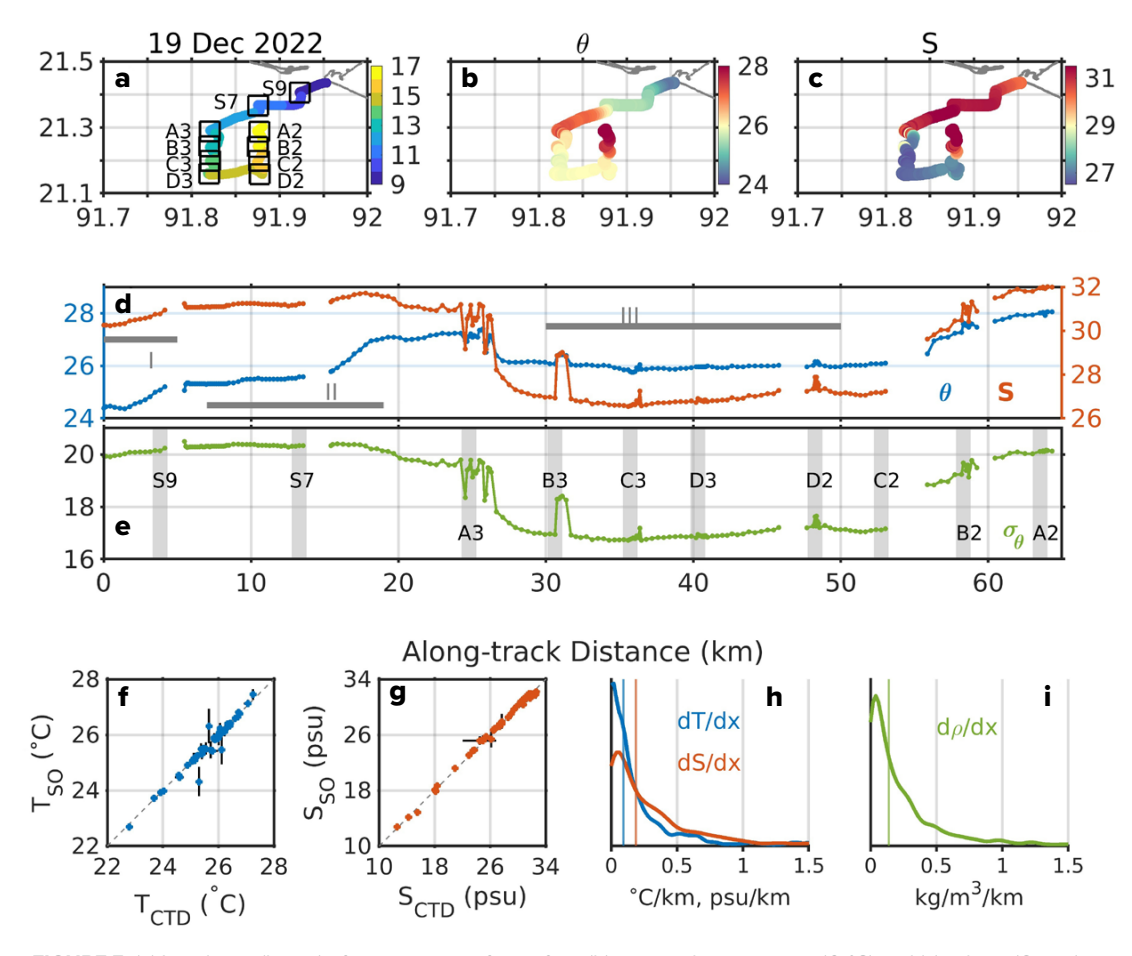


**FIGURE 5.** (a) Local time (hours) of measurement for surface (b) potential temperature ( $\theta$ ; °C) and (c) salinity (S; psu) data collected on December 19, 2022, from a fishing boat. Open squares (black) show the locations of ten CTD stations. Surface (d) potential temperature (blue) and salinity (red), and (e) potential density (green) are plotted along the boat's track. The three horizontal lines (gray) in panel (d) represent three different types of water mass (I, II, and III). (f,g) Scatterplots show temperature (f) and salinity (g) as measured by a Star-Oddi sensor ( $T_{SO}$ ) within a 10-minute window, centered around each CTD profile ( $T_{CTD}$ ), averaged over the depth range of 0–2 m. The error bars represent one standard deviation of the measurements. Dashed lines in panels a and b represent the 1:1 line. Probability density functions (PDFs) for (h) the horizontal salinity  $\frac{dS}{dx}$ , psu, red) and temperature absolute gradients ( $\frac{dT}{dx}$ , °C, blue) and (i) the potential density absolute gradient ( $\frac{dp}{dx}$ , kg m<sup>-3</sup>, green) collected along the boat tracks during five days of coastal measurements. The gray vertical lines in panel e mark the CTD stations along the boat track. The blue, red, and green vertical lines in panels (h) and (i) mark the median of the probability density functions for the horizontal potential temperature, salinity, and potential density gradients.

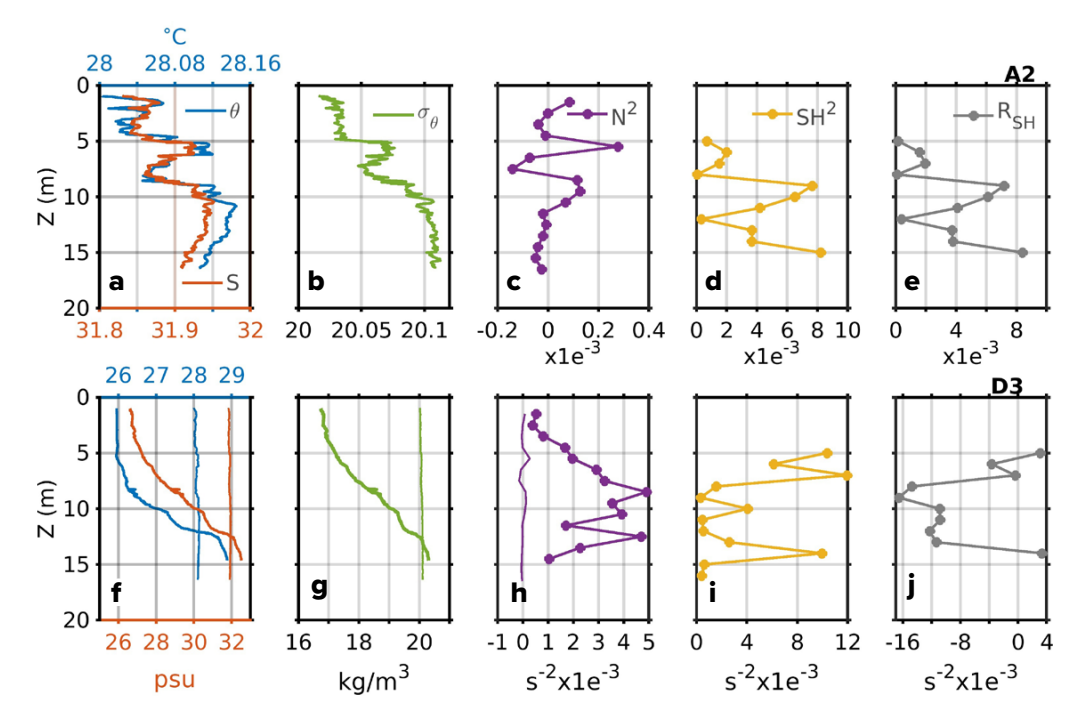


**FIGURE 6.** Plots show profiles of (a,f) potential temperature ( $\theta$ , blue, °C) and salinity (S, red; psu), (b,g) potential density ( $\sigma_{\theta}$ , green, kg m<sup>-3</sup>), (c,h) square of the Brunt-Väisälä buoyancy frequency ( $N^2$ , maroon, s<sup>-2</sup>), (d,i) square of the shear ( $SH^2$ , yellow, s<sup>-2</sup>), and (e,j) reduced shear ( $SH^2$ -4 $N^2$ , gray). Thin lines in panels f, g, and h represent similar quantities, but in panels a, b, and c.

the presence of submesoscale fronts in this region, consistent with previous studies conducted in the open bay (Sengupta et al., 2016; Jaeger and Mahadevan, 2018). The magnitude of the lateral gradient of temperature, salinity, and potential density along the boat track exceeds 0.05 l/km ( $l \equiv {}^{\circ}C$ , psu, kg m<sup>-3</sup>) about 15%, 25%, and 19% of the time (Figure 5h,i).

### VERTICAL STRATIFICATION AND SHEAR

Temperature and salinity profiles have been plotted at selected locations A2, near the coast, and D3, at the front, (both indicated in Figure 5a) along the track (Figure 6) to illustrate the vertical structure and variability of the upper ocean. The D3 profile displays a double pycnocline structure, with peaks in the vertical density gradient occurring between depths of 6 m and 8 m and 11 m and 13 m (Figure 6h). This vertical density gradient is stabilized by a salinity gradient as riverine water creates a salinity difference of 5 psu between the surface and bottom layers (Figure 6f). This stabilization counteracts the destabilizing effect of the temperature gradient, where the surface layer is 4°C colder than the warmer subsurface layer (Figure 6f). Such a temperature inversion is commonly observed in the Bay of Bengal during winter (Thadathil et al., 2016; Vinayachandran et al., 2002; Masud-Ul-Alam et al., 2022).

In contrast, the A2 profile represents a relatively well-mixed layer (**Figure 6a**). A negative Brunt-Väisälä buoyancy frequency squared value  $N^2$  in the depth range of 5–8 m (**Figure 6c**) indicates a vertical density overturn, suggesting substantial vertical mixing near the coast (**Figure 6b**). The estimations of reduced shear  $(R_{SH} = SH^2 - 4N^2)$  further support these observations. A reduced-shear value greater than zero ( $R_{SH} > 0$ ) indicates active turbulence, while a value less than zero ( $R_{SH} < 0$ ) suggests a lack of turbulence. **Figure 6e,j** shows that strong stratification resists significant shear, contributing to the stability of the D3 profile, whereas shear-induced mixing and weak stratification lead to a well-mixed layer at A2. Notably, both profiles exhibit partially vertically compensated water masses.

# **DISCUSSION**

Co-located measurements of temperature, salinity, and horizontal velocity provide valuable insights into the variability of temperature and salinity and the vertical shear structure in Bangladesh's coastal waters. The vertical resolution of the data ranges from 0.25 m to 1 m, while the horizontal resolution averages around 300 m, sufficient to capture submesoscale features (1–20 km).

The study reveals the presence of sharp, salinity-dominated near-surface density fronts that are sometimes partially compen-

<sup>&</sup>lt;sup>2</sup> The Richardson number criterion, defined as  $\frac{N^2}{SH^2}$  < 0.25, is often used to identify mixing events in the ocean. Reduced shear, derived from the above criterion, is expressed as  $SH^2 - 4N^2$ . If this value is positive, it means that the shear is strong enough to cause mixing. If the value is negative, it indicates that the stratification is stronger, allowing the layers to remain stable.

sated by temperature differences. The largest gradient exceeds 4 kg m<sup>-3</sup> over a distance of 4 km. Furthermore, the data indicate large temperature inversions, which are common in the open bay during winter.

The findings also highlight the complex pathways and mixing patterns of river water in the ocean. For example, a narrow 10 km-wide coastal jet transports salty water into the northern BoB shelves, maintaining the salt balance. We hypothesize that this jet is a seasonal phenomenon occurring in winter, which helps prevent the shelves from becoming fresher.

coastal conditions, create a regional ocean model for the northern BoB, and help restore coral habitats.

We have succeeded in two main areas. The first area of success encompasses the development of an indigenous method for measuring coastal oceans with modern sensors and the collection of unprecedented data in uncharted waters by Bangladeshi scientists. There are three key reasons for this success. (1) Instead of developing low-cost sensors, BORI initially purchased modern instruments, thanks to initial government funding of \$50,000. (2) BORI also offered support in terms of logistics, operations, and infra-

The second area of success is that, from an oceanographic perspective, our work provides unique insights into the rich upper-ocean temperature-salinity variability and vertical shear structure in Bangladesh's coastal waters.

To illustrate these concepts, we can consider an idealized budget for salt mixing expressed as

$$\frac{dS}{dt} = \frac{F_V}{\Lambda S} \tag{1}$$

where  $\frac{dS}{dt}$  is the overall change in salinity on the shelf,  $F_V = vh_2w$ is the volume flow, v is the meridional velocity,  $h_2$  is depth, w is width,  $\Delta S = S_I - S_F$ ,  $S_I$  is the salinity of the BoB,  $S_F$  is the salinity of the shelf sea, and  $V_{\rm S}$  is the volume of the shelf where the depth is less than 10 m (see Figure 3e). Our measurements indicate that  $v = 0.5 \text{ m s}^{-1}$ ,  $h_2 = 20 \text{ m}$ , w = 10 km,  $V_S = 9 \times 10^9 \text{ m}^3$ ,  $S_I = 32$  psu, and  $S_F = 12$  psu (see Figure 3). By substituting these values into Equation 1, we estimate that  $\frac{dS}{dt}$  is 2 psu/day, suggesting that the shelf water rapidly freshens by mixing with water from the local rivers as it moves northward. More generally, this suggests that many of the properties of the shelf water—salinity, oxygen, nutrient concentration, and plankton—are strongly influenced by similar balances between open ocean and riverine inputs, and that these might change rapidly as this balance shifts due to variations in either input or the mixing rate. We can explore this hypothesis in future studies.

#### CONCLUSIONS

The northern shelves of the BoB associated with the mouth of the Ganga-Brahmaputra-Meghna Rivers are among the least sampled areas in the upper ocean. The establishment of BORI in 2018, along with the goals set by the Bangladesh government, marked a significant step toward a systematic scientific observation program. This initiative aligns with the country's vision of a blue economy by 2028, focusing on collecting data on the physical, chemical, biological, and geological aspects of the ocean. It will also monitor

structure development by setting up laboratories and data centers, ensuring the long-term success of our coastal observation programs. (3) Collaboration between oceanographers from BORI and the Applied Physics Laboratory, University of Washington, in buying instruments, designing experiments, and processing data played an important role in our success. This enthusiasm and eagerness, bolstered by expert training, will pave the way for "cost-conscious oceanography," a new frontier for developing countries in the Global South that cannot afford expensive ocean observation programs. Similar future observational efforts will help address data gaps in many areas of the global ocean, ultimately aiding in more accurate sea predictions.

The second area of success is that, from an oceanographic perspective, our work provides unique insights into the rich upper-ocean temperature-salinity variability and vertical shear structure in Bangladesh's coastal waters. These findings suggest complex pathways and mixing patterns of river water in the ocean. Ongoing efforts to collect additional variables, such as oxygen, chlorophyll, turbidity, and tides, are explicitly important for the effective management of coastal resources.

#### **REFERENCES**

Balaguru, K., P. Chang, R. Saravanan, L.R. Leung, Z. Xu, M. Li, and J.-S. Hsieh. 2012. Ocean barrier layers' effect on tropical cyclone intensification. *Proceedings of the National Academy of Sciences of the United States of America* 109(36): 14,343–14,347, https://doi.org/10.1073/pnas.1201364109.

Balaguru, K., S. Taraphdar, L.R. Leung, and G.R. Foltz. 2014. Increase in the intensity of postmonsoon Bay of Bengal tropical cyclones. *Geophysical Research Letters* 41(10):3,594–3,601, <a href="https://doi.org/10.1002/2014GL060197">https://doi.org/10.1002/2014GL060197</a>.

Bhat, G.S., S. Gadgil, P.V. Hareesh Kumar, S.R. Kalsi, P. Madhusoodanan, V.S.N. Murty, C.V.K. Prasada Rao, V. Ramesh Babu, L.V.G. Rao, R.R. Rao, and others. 2001. BOBMEX: The Bay of Bengal Monsoon Experiment. *Bulletin of the American Meteorological Society* 82(10):2,217–2,244, https://doi.org/10.1175/1520-0477(2001) 082<2217:BTBOBM>2.3.CO;2.

- Boutin, J., N. Reul, J. Koehler, A. Martin, R. Catany, S. Guimbard, F. Rouffi, J.L. Vergely, M. Arias, M. Chakroun, and others. 2021. Satellite-based sea surface salinity designed for ocean and climate studies. *Journal of Geophysical Research:*Oceans 126(11):e2021JC017676, <a href="https://doi.org/10.1029/2021JC017676">https://doi.org/10.1029/2021JC017676</a>.
- Chaudhuri, D., D. Sengupta, E. D'Asaro, R. Venkatesan, and M. Ravichandran. 2019. Response of the salinity-stratified Bay of Bengal to Cyclone Phailin. *Journal of Physical Oceanography* 49(5):1,121–1,140, https://doi.org/10.1175/JPO-D-18-0051.1.
- Chaudhury, A.B.R., and H.V. Pant, eds. 2024. *Anchoring the Bay of Bengal in a Free and Open Indo-Pacific*. Global Policy (GP E-Books).
- Dimri, A.P., and A. Chevuturi. 2016. Western disturbances—Indian seasons.
  Pp. 61–82 in Western Disturbances—An Indian Meteorological Perspective.
  Springer International Publishing, Cham, <a href="https://doi.org/10.1007/978-3-319-26737-1">https://doi.org/10.1007/978-3-319-26737-1</a>.
- Donlon, C., I. Robinson, K.S. Casey, J. Vasquez-Cuervo, E. Armstrong, O. Arino, C. Gentemann, D. May, P. LeBorgne, J. Piollé, and others. 2007. The global ocean data assimilation experiment high-resolution sea surface temperature pilot project. *Bulletin of the American Meteorological Society* 88(8):1,197–1,214, https://doi.org/10.1175/BAMS-88-8-1197.
- Flament, P. 2002. A state variable for characterizing water masses and their diffusive stability: Spiciness. *Progress in Oceanography* 54(1):493–501, <a href="https://doi.org/10.1016/S0079-6611(02)00065-4">https://doi.org/10.1016/S0079-6611(02)00065-4</a>.
- Garcia, H.E., T.P. Boyer, O.K. Baranova, R.A. Locarnini, A.V. Mishonov, A. Grodsky, C.R. Paver, K.W. Weathers, I.V. Smolyar, J.R. Reagan, and others. 2019. *World Ocean Atlas 2018: Product Documentation*. A. Mishonov, technical ed., <a href="https://www.ncei.noaa.gov/data/oceans/woa/WOA18/DOC/woa18documentation.pdf">https://www.ncei.noaa.gov/data/oceans/woa/WOA18/DOC/woa18documentation.pdf</a>.
- Goswami, B.N. 2012. South Asian monsoon. Pp. 21–72 in Intraseasonal Variability in the Atmosphere-Ocean Climate System, 2nd ed. W.K.M. Lau and D.E. Waliser, eds, Springer, https://doi.org/10.1007/978-3-642-13914-7\_2.
- Jackett, D.R., and T.J. McDougall. 1985. An oceanographic variable for the characterization of intrusions and water masses. *Deep Sea Research Part A* 32(10): 1,195–1,207, https://doi.org/10.1016/0198-0149(85)90003-2.
- Jaeger, G.S., and A. Mahadevan. 2018. Submesoscale-selective compensation of fronts in a salinity-stratified ocean. Science Advances 4(2), <a href="https://doi.org/10.1126/sciadv.1701504">https://doi.org/10.1126/sciadv.1701504</a>.
- Masud-Ul-Alam, M., M.A.I. Khan, B.S. Barrett, S. Rivero-Calle, M.R. Golder, and M.A. Rouf. 2022. Spatial variability of the winter thermal inversion in the northern Bay of Bengal. *Regional Studies in Marine Science* 53:102417, https://doi.org/ 10.1016/j.rsma.2022.102417.
- McPhaden, M.J., G. Meyers, K. Ando, Y. Matsumoto, V.S.N. Murty, M. Ravichandran, F. Syamsudin, J. Vialard, L. Yu, and W. Yu. 2009. RAMA: The research moored array for African-Asian-Australian monsoon analysis and prediction. *Bulletin of the American Meteorological Society* 90(4):459–480, <a href="https://doi.org/10.1175/2008BAMS2608.1">https://doi.org/10.1175/2008BAMS2608.1</a>.
- Neetu, S., M. Lengaigne, E.M. Vincent, J. Vialard, G. Madec, G. Samson, M. Ramesh Kumar, and F. Durand. 2012. Influence of upper-ocean stratification on tropical cyclone-induced surface cooling in the Bay of Bengal. *Journal of Geophysical Research: Oceans* 117(C12), https://doi.org/10.1029/2012JC008433.
- Pearson, K., C. Merchant, O. Embury, and C. Donlon. 2018. The role of advanced microwave scanning radiometer 2 channels within an optimal estimation scheme for sea surface temperature. *Remote Sensing* 10(1):90, <a href="https://doi.org/10.3390/rs10010090">https://doi.org/10.3390/rs10010090</a>.
- Ranjan, A., and C. Attanayake. 2024. The Bay of Bengal in the evolving Indo-Pacific debate. *Australian Journal of Maritime & Ocean Affairs* 16(3):285–291, https://doi.org/10.1080/18366503.2024.2383820.
- Roemmich, D., G.C. Johnson, S. Riser, R. Davis, J. Gilson, W.B. Owens, S.L. Garzoli, C. Schmid, and M. Ignaszewski. 2009. The Argo program: Observing the global ocean with profiling floats. *Oceanography* 22(2):34–43, <a href="https://doi.org/10.5670/oceanog.2009.36">https://doi.org/10.5670/oceanog.2009.36</a>.
- Samanta, D., S.N. Hameed, D. Jin, V. Thilakan, M. Ganai, S.A. Rao, and M. Deshpande. 2018. Impact of a narrow coastal Bay of Bengal sea surface temperature front on an Indian summer monsoon simulation. *Scientific Reports* 8:17694, <a href="https://doi.org/10.1038/s41598-018-35735-3">https://doi.org/10.1038/s41598-018-35735-3</a>.
- Sengupta, D., G. Bharath Raj, and S. Shenoi. 2006. Surface freshwater from Bay of Bengal runoff and Indonesian throughflow in the tropical Indian Ocean. Geophysical Research Letters 33(22), https://doi.org/10.1029/2006GL027573.
- Sengupta, D., B.R. Goddalehundi, and D. Anitha. 2008. Cyclone-induced mixing does not cool SST in the post-monsoon North Bay of Bengal. Atmospheric Science Letters 9(1):1–6, https://doi.org/10.1002/asl.162.
- Sengupta, D., G. Bharath Raj, M. Ravichandran, J. Sree Lekha, and F. Papa. 2016. Near-surface salinity and stratification in the north Bay of Bengal from moored observations. *Geophysical Research Letters* 43(9):4,448–4,456, <a href="https://doi.org/10.1002/2016GL068339">https://doi.org/10.1002/2016GL068339</a>.
- Shroyer, E., A. Tandon, D. Sengupta, H.J.S. Fernando, A.J. Lucas, J.T. Farrar, R. Chattopadhyay, S. de Szoeke, M. Flatau, A. Rydbeck, and others. 2021. Bay of Bengal intraseasonal oscillations and the 2018 monsoon onset. *Bulletin of the American Meteorological Society* 102(10):E1936–E1951, <a href="https://doi.org/10.1175/BAMS-D-20-0113.1">https://doi.org/10.1175/BAMS-D-20-0113.1</a>.

- Thadathil, P., I. Suresh, S. Gautham, S. Prasanna Kumar, M. Lengaigne, R. Rao, S. Neetu, and A. Hegde. 2016. Surface layer temperature inversion in the Bay of Bengal: Main characteristics and related mechanisms. *Journal of Geophysical Research: Oceans* 121(8):5,682–5,696, https://doi.org/10.1002/2016JC011674.
- Venkatesan, R., V. Shamji, G. Latha, S. Mathew, R. Rao, A. Muthiah, and M. Atmanand. 2013. In situ ocean subsurface time-series measurements from OMNI buoy network in the Bay of Bengal. *Current Science* 104(9):1,166–1,177.
- Vinayachandran, P., V. Murty, and V. Ramesh Babu. 2002. Observations of barrier layer formation in the Bay of Bengal during summer monsoon. *Journal of Geophysical Research: Oceans* 107(C12), https://doi.org/10.1029/2001JC000831.
- Waliser, D., K. Jin, I.-S. Kang, W.F. Stern, D. Schubert, M.L.C. Wu, K.-M. Lau, M.-I. Lee, V. Krishnamurthy, A. Kitoh, and others. 2003. AGCM simulations of intraseasonal variability associated with the Asian summer monsoon. *Climate Dynamics* 21(5–6):423–446, https://doi.org/10.1007/s00382-003-0337-1.
- Wentz, F.J., C. Gentemann, D. Smith, and D. Chelton. 2000. Satellite measurements of sea surface temperature through clouds. *Science* 288(5467):847–850, https://doi.org/10.1126/science.288.5467.847.
- Wijesekera, H.W., E. Shroyer, A. Tandon, M. Ravichandran, D. Sengupta, S.U.P. Jinadasa, H.J.S. Fernando, N. Agrawal, K. Arulananthan, G.S. Bhat, and others. 2016. ASIRI: An ocean-atmosphere initiative for Bay of Bengal. *Bulletin of the American Meteorological Society* 97(10):1,859–1,884, https://doi.org/10.1175/BAMS-D-14-00197.1.

#### **ACKNOWLEDGMENTS**

This work was supported by Research and Development grants from the Bangladesh Oceanographic Research Institute, Ministry of Science and Technology. Work by DC and EAD is supported by Office of Naval Research Grants N00014-17-1-2728 and N00014-23-1-2216. We thank all members of the BORI team for their excellent cooperation in obtaining the measurements. DC expresses gratitude to Debasis Sengupta for insightful discussion. Additionally, DC appreciates EAD for supporting travel from the United States to Bangladesh. Lastly, DC thanks BORI for hosting and providing the opportunity to engage in this exceptional collaborative effort.

#### **AUTHORS**

Rupak Loodh, Bangladesh Oceanographic Research Institute, Cox's Bazar,
Bangladesh. Dipanjan Chaudhuri (dipadadachaudhuri@gmail.com), Applied Physics
Laboratory, University of Washington, Seattle, WA, USA. Eric D'Asaro, Applied Physics
Laboratory and School of Oceanography, University of Washington, Seattle, WA, USA.
Md Minarul Hoque, Bangladesh Oceanographic Research Institute, Cox's Bazar,
Bangladesh.

## ARTICLE CITATION

Loodh, R., D. Chaudhuri, E. D'Asaro, and M.M. Hoque. 2025. Cost-conscious measurements in the coastal waters of Bangladesh. *Oceanography* 38(4), https://doi.org/10.5670/oceanog.2025.e403.

### **COPYRIGHT & USAGE**

This is an open access article made available under the terms of the <u>Creative Commons Attribution 4.0 International License</u>, which permits use, sharing, adaptation, distribution, and reproduction in any medium or format as long as users cite the materials appropriately, provide a link to the Creative Commons license, and indicate the changes that were made to the original content.